JOURNAL OF SOLID STATE CHEMISTRY **133,** 416–422 (1997)
ARTICLE NO. SC977500

Formation of Copper–Manganese Oxides from $Cu_xMn_{1-x}(HCOO)_2 \cdot 2H_2O$ Mixed Crystals

V. Koleva, D. Stoilova,[1] and D. Mehandjiev

Institute of General and Inorganic Chemistry, Bulgarian Academy of Sciences, Sofia 1113, Bulgaria

Received March 26, 1997; in revised form May 23, 1997; accepted May 28, 1997

It has been established that two series of mixed crystals are formed in the $Cu(HCOO)_2$–$Mn(HCOO)_2$–$2H_2O$ system at 25°C. The thermal decompositions of $Cu_xMn_{1-x}(HCOO)_2 \cdot 2H_2O$ mixed crystals ($0 \leq x \leq 0.5$) have been studied. On the basis of the methods used (TG, DTA, and X-ray diffraction analysis), it has been established that homogeneous and heterogeneous oxide phases are obtained depending on the x-values. At about 300°C the formates decompose to Mn_5O_8 ($x = 0$); $Cu_{0.4}Mn_{4.6}O_8$ ($x = 0.08$); a mixture of $Cu_{0.4}Mn_{4.6}O_8$ and $Cu_{1.5}Mn_{1.5}O_4$ with a different ratio ($0.08 < x < 0.5$), and a $Cu_{1.5}Mn_{1.5}O_4$ spinel ($x = 0.5$). $Cu_{0.4}Mn_{4.6}O_8$ ($Cu^{2+}_{0.4}Mn^{2+}_{0.4}Mn^{4+}_3O_8$) crystallizes in the monoclinic system with lattice parameters $a = 10.39(1)$ Å, $b = 5.729(4)$ Å, $c = 4.862(5)$ Å, $\beta = 109.4°$ and space group $C2/m$. At about 600°C the oxides obtained transform into α-Mn_2O_3 ($x = 0$) and a mixture of α-Mn_2O_3 and $Cu_{1.5}Mn_{1.5}O_4$ with a different ratio ($0 < x < 0.5$). The slowly cooled specimen shows a fine structure in the IR spectrum due to the 1 : 3 ordering of the ions on the B-sublattice, and the cation valences are $Cu^+[Cu^{2+}_{0.5}Mn^{4+}_{4.5}]O_4$. The magnetic measurements show that the oxides obtained are paramagnetic in the temperature range of 25–300°C, and the $1/\chi$ versus T curves obey the Curie–Weiss law. The theoretical and experimental magnetic moments of the oxides are given. They coincide well in the case of the homogeneous samples.

INTRODUCTION

It is well known that the pure and mixed oxides of copper and manganese are widely used as active materials for many catalytic reactions. Manganese nitrate has been used in the preparation of supported catalysts in nearly all studies, probably because of its high solubility and the ease of removal of the nitrate anion during calcination. However, it has been recently shown that the preparation of alumina-supported manganese oxide catalysts with manganese acetate as precursor results in a highly dispersed oxide phase, homogeneously distributed throughout the alumina particles (1, 2). The $Cu(HCOO)_2/Mn(HCOO)_2$ system has not been studied as a precursor in the preparation of oxides. The formates of copper and manganese decompose to the corresponding oxides at comparatively low temperatures (about 350–400°C). On the other hand, the isostructural dihydrates of the copper and manganese formates form mixed crystals during their cocrystallization from aqueous solutions (3). It is expected that the thermal decompositions of the homogeneous mixed formate crystals will lead to the formation of mixed oxides with a highly dispersion and catalytic activity.

In connection with our investigations of the preparation of alumina-supported copper–manganese oxide catalysts the aim of this paper is the study on the thermal decompositions of mixed copper–manganese formates.

EXPERIMENTAL

The metal formates were prepared by neutralization of dilute formic acid solutions with the corresponding hydroxide carbonates at 70–80°C. The solutions were then filtered and concentrated. The crystals grew by cooling at room temperature and were then recrystallized from water and dried in air. The reagents used were “p.a.” (Merck). The mixed copper manganese formates were prepared by crystallization from mixed solutions with a different ratio of the salts. The solubility in the $Cu(HCOO)_2$–$Mn(HCOO)_2$–$2H_2O$ system was studied using the method described in ref. (4).

The thermal dehydration and decomposition of the mixed crystals were studied using a derivatograph Paulik–Paulik–Erdey MOM OD-102 in the temperature range up to 800°C at a heating rate of 10°C min^{-1} using α-alumina as a reference material (sample mass 150 mg). The X-ray diffraction analysis was carried out by means of a DRON-3 powder diffractometer using CuKα radiation at a scanning speed of 1° min^{-1}. The measurements were performed in a 2θ diffraction range of 8–70°. The lattice parameters were calculated using the program LSUCR. The infrared spectra were recorded on Brucker model IFS 25

---

[1] To whom correspondence should be addressed.

0022-4596/97 $25.00

Fourier transform interferometer (resolution $<2\ cm^{-1}$) using KBr discs as matrices. Ion exchange or other reactions with KBr have not been observed. The magnetic susceptibility was determined per gram sample by means of a Faraday type magnetic balance at a temperature range of 25–300°C. The copper content in the liquid and solid phases was determined iodometrically. Mn^{2+} concentration was determined complexometrically after masking the Cu^{2+} ions with KCN. The higher oxidation state of manganese was determined using the Bunzen–Rupp method (5–7).

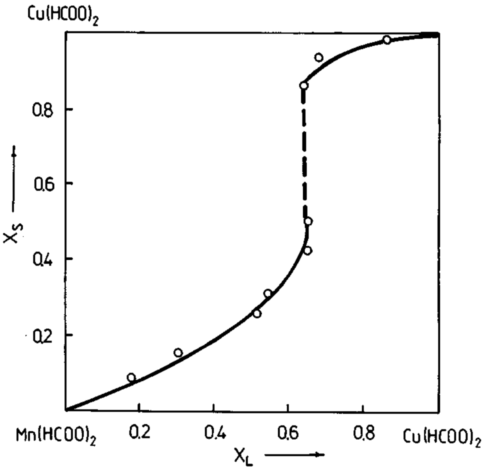

FIG. 1. Distribution curve of the salt components in the $Cu(HCOO)_2$–$Mn(HCOO)_2$–H_2O system at 25°C.

RESULTS AND DISCUSSION

For the solubilities in the $Cu(HCOO)_2$–$Mn(HCOO)_2$–$2H_2O$ system at 25°C see Table 1. The distribution curve of the salt components (in molar parts) is shown in Fig. 1. The data show that two series of mixed crystals are formed in the system: one series having $Mn(HCOO)_2 \cdot 2H_2O$ as a matrix and the other having $Cu(HCOO)_2 \cdot 4H_2O$ as a matrix. A mixture of the two series of mixed crystals is formed within the concentration range limited by the broken line (eutonic area $0.86 \geq x \geq 0.5$). On the basis of the IR and X-ray studies it has been established that when mixed crystals are formed between the manganese and copper formates at 50°C the two metal ions are localized preferentially on one of the two metal positions in the $Mn(HCOO)_2 \cdot 2H_2O$ crystal structure and Cu^{2+} ions occupy the Me(I) sites, coordinated by formate groups only (3). The same lattice parameters and the identical IR spectra of the $Cu_xMn_{1-x}(HCOO)_2 \cdot 2H_2O$ mixed crystals obtained at 25 and 50°C are evidence of the same metal ion distribution in the crystals at both temperatures.

The simultaneous obtained TG, DTA, and DTG curves for $Mn(HCOO)_2 \cdot 2H_2O$ and the mixed crystals having the manganese formate dihydrate as a matrix are shown in Fig. 2. The X-ray patterns of the oxide systems obtained by heating of the formate samples at 440 and 620°C for several hours are shown in Figs. 3 and 4. The X-ray and IR measurements show that in 2 h the mixed crystals decompose completely, forming the corresponding oxides.

A strong endothermic DTA peak with a maximum at 140°C corresponds to the separation of two water molecules thus transforming $Mn(HCOO)_2 \cdot 2H_2O$ into an anhydrous salt which is stable in the temperature interval from 140 to 220°C (Fig. 2a). At temperatures higher than 220°C the manganese formate dihydrate begins to decompose, and the decomposition processes are registered on the DTA curve with a series of exothermic peaks at about 220, 300, and 380°C. According to other studies MnO (8, 9), Mn_2O_3 (10), or Mn_3O_4 (11) are produced as a result of the thermal

TABLE 1
Solubility in the $Cu(HCOO)_2$–$Mn(HCOO)_2$–H_2O System at 25°C

Liquid phase, wt%		Solid phase, wt%				Composition of the solid phase
MnF	CuF	MnF	CuF	$D_{Cu/Mn}$[a]	$D_{Mn/Cu}$[a]	
6.28	—	—	—	—	—	$Mn(HCOO)_2 \cdot 2H_2O$
6.40	1.50	57.13	5.26	0.37	2.70	$Cu_{0.08}Mn_{0.92}(HCOO)_2 \cdot 2H_2O$
6.18	2.90	49.16	9.76	0.39	2.56	$Cu_{0.15}Mn_{0.85}(HCOO)_2 \cdot 2H_2O$
5.43	4.64	38.41	14.34	0.40	2.50	$Cu_{0.25}Mn_{0.75}(HCOO)_2 \cdot 2H_2O$
5.01	6.02	31.08	16.05	0.38	2.63	$Cu_{0.30}Mn_{0.70}(HCOO)_2 \cdot 2H_2O$
4.40	8.50	36.03	29.51	0.40	2.50	$Cu_{0.43}Mn_{0.57}(HCOO)_2 \cdot 2H_2O$
4.39	8.60	36.50	38.35	—	—	Eutonics
4.47	8.63	8.17	50.81	3.45	0.29	$Cu_{0.86}Mn_{0.14}(HCOO)_2 \cdot 4H_2O$
3.64	8.36	4.00	56.10	6.67	0.15	$Cu_{0.94}Mn_{0.06}(HCOO)_2 \cdot 4H_2O$
1.29	8.37	0.57	58.80	20.00	0.05	$Cu_{0.01}Mn_{0.99}(HCOO)_2 \cdot 4H_2O$
—	8.80	—	—	—	—	$Cu(HCOO)_2 \cdot 4H_2O$

[a] *D*, distribution coefficients of the salt components between the liquid and solid phases.

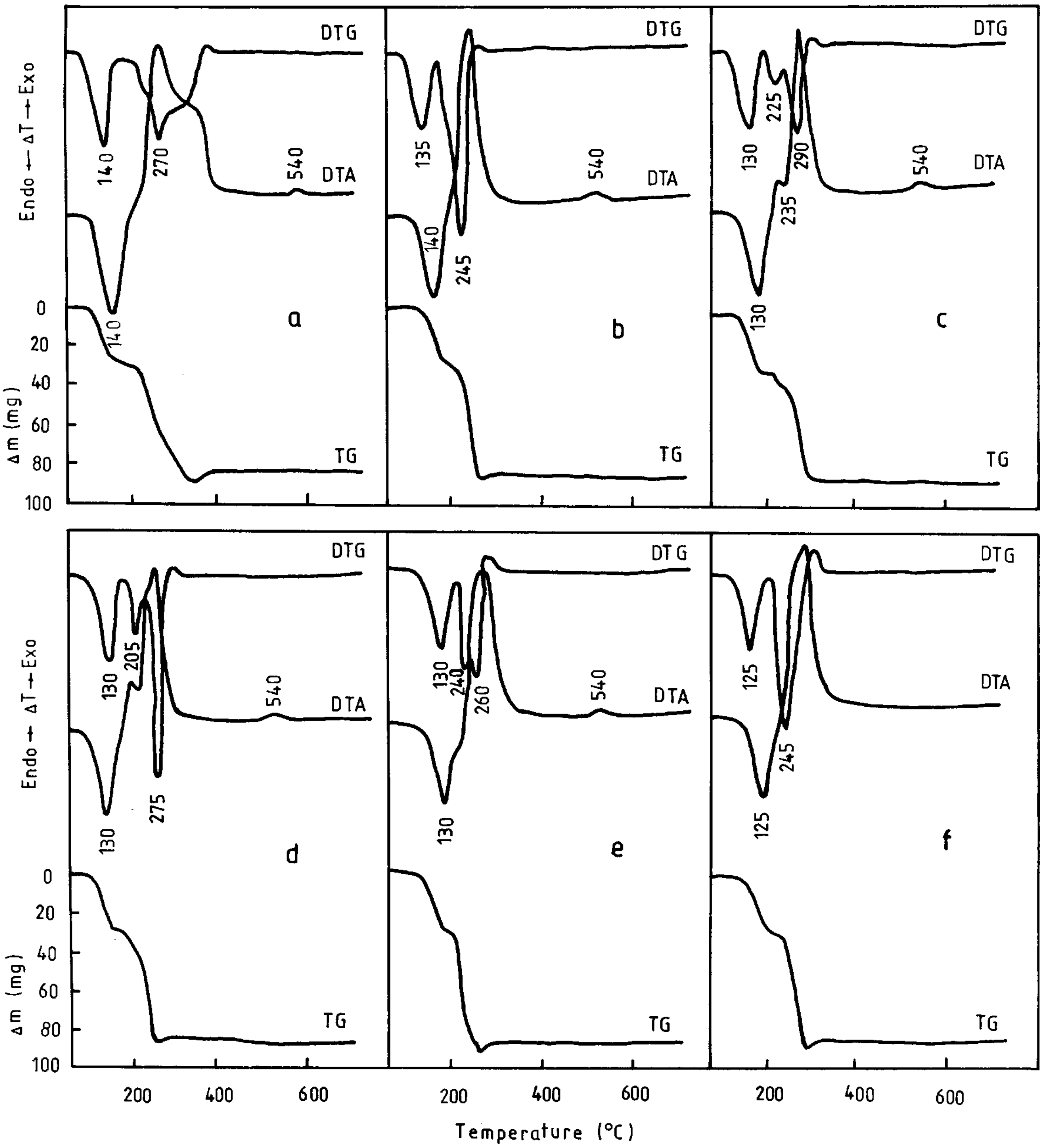

FIG. 2. TG, DTG, and DTA curves of $Mn(HCOO)_2 \cdot 2H_2O$ (a); $Cu_{0.08}Mn_{0.92}(HCOO)_2 \cdot 2H_2O$ (b); $Cu_{0.25}Mn_{0.75}(HCOO)_2 \cdot 2H_2O$ (c); $Cu_{0.30}Mn_{0.70}(HCOO)_2 \cdot 2H_2O$ (d); $Cu_{0.43}Mn_{0.57}(HCOO)_2 \cdot 2H_2O$ (e); and $Cu_{0.5}Mn_{0.5}(HCOO)_2 \cdot 2H_2O$ (f).

decomposition of the manganese formate dihydrate in air at about 400°C. However, our X-ray powder diffraction studies show that Mn_5O_8 [$Mn_2^{2+}Mn_3^{4+}O_8$] is formed in the temperature interval from 400 to 540°C (Fig. 3a). The calculated lattice parameters of Mn_3O_8 are $a = 10.392(4)$ Å, $b = 5.727(2)$ Å, $c = 4.860(2)$ Å, and $\beta = 109.6°$, space group $C2/m$, and they are very close to those given by Ostwald *et al.* (12). The small exothermic effect at 560°C on the DTA curve (Fig. 2a) corresponds to the transformation of Mn_5O_8 into α-Mn_2O_3 with a lattice parameter $a = 9.404(1)$ Å which coincides with that reported in ref. (13).

In the case of the $Cu_{0.08}Mn_{0.92}(HCOO)_2 \cdot 2H_2O$ mixed crystal, the corresponding anhydrous salt is stable in a narrower temperature interval (140–160°C) than Mn $(HCOO)_2 \cdot 2H_2O$ and the decomposition process is complete at about 300°C (Fig. 2b) with the formation of $Cu_{0.4}Mn_{1.6}Mn_3O_8$ (Fig. 3b). It crystallizes in the monoclinic system with lattice parameters $a = 10.39(1)$ Å, $b = 5.729(4)$ Å, $c = 4.862(5)$ Å, and $\beta = 109.4°$, which are close to those of the pure Mn_5O_8. The X-ray pattern of the above mixed crystal heated at 620°C shows that the homogeneous oxide phase transforms into two phases: α-Mn_2O_3 and

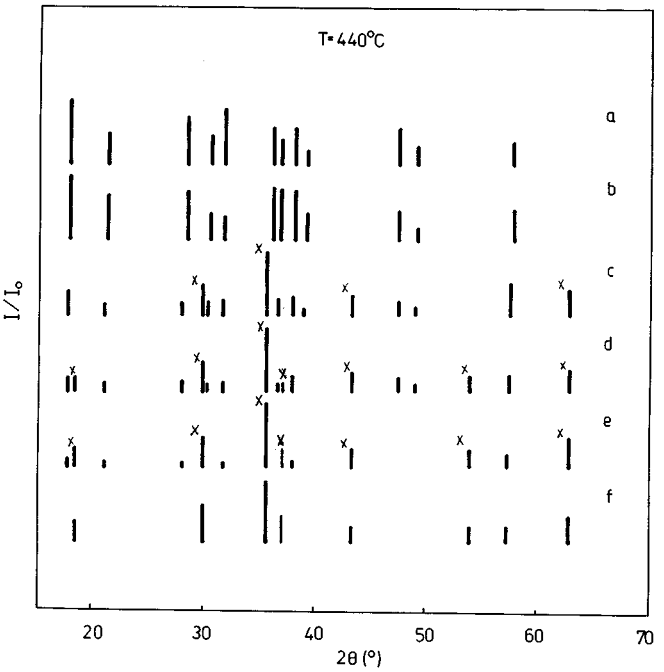

FIG. 3. Stick diagrams due to the X-ray reflections of the oxides obtained at 440°C: Mn_5O_8 (a); $Cu_{0.4}Mn_{1.6}Mn_3O_8$ (b); $Cu_{0.4}Mn_{1.6}Mn_3O_8 + Cu_{1.5}Mn_{1.5}O_4$ (0.88 : 1) (c); $Cu_{0.4}Mn_{1.6}Mn_3O_8 + Cu_{1.5}Mn_{1.5}O_4$ (0.54 : 1) (d); $Cu_{0.4}Mn_{1.6}Mn_3O_8 + Cu_{1.5}Mn_{1.5}O_4$ (0.12 : 1) (e); $Cu_{1.5}Mn_{1.5}O_4$ (f). Reflections labeled with "*" are from $Cu_{1.5}Mn_{1.5}O_4$, and nonlabeled reflections are from $Cu_{0.4}Mn_{1.6}Mn_3O_8$ in the mixture of oxides.

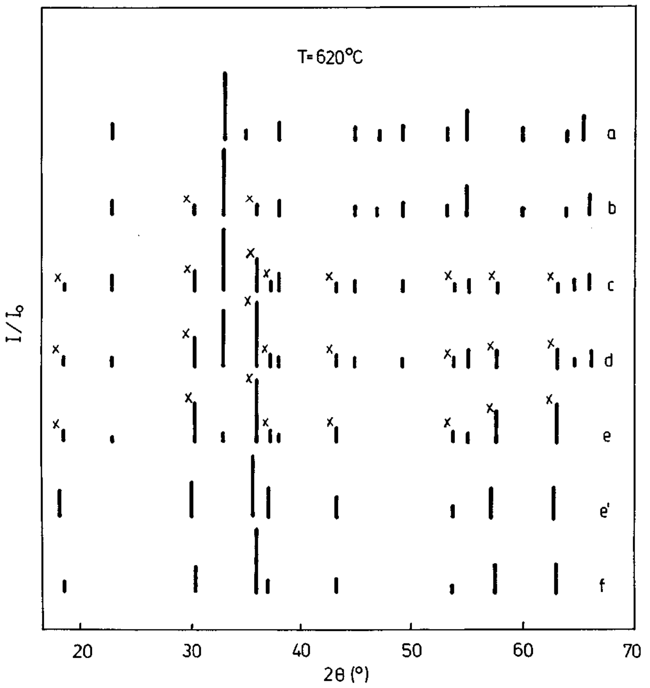

FIG. 4. Stick diagrams due to the X-ray reflections of the oxides obtained at 620°C: α-Mn_2O_3 (a); α-$Mn_2O_3 + Cu_{1.5}Mn_{1.5}O_4$ (1 : 0.13) (b); α-$Mn_2O_3 + Cu_{1.5}Mn_{1.5}O_4$ (1 : 0.66) (c); α-$Mn_2O_3 + Cu_{1.5}Mn_{1.5}O_4$ (1 : 1) (d); α-$Mn_2O_3 + Cu_{1.5}Mn_{1.5}O_4$ (1 : 4.1) (e); $Cu_{1.27}Mn_{1.73}O_4$ (e'); $Cu_{1.5}Mn_{1.5}O_4$ (f). Reflections labeled with "*" are from $Cu_{1.5}Mn_{1.5}O_4$, and nonlabeled reflections are from α-Mn_2O_3 in the mixture of oxides.

$Cu_{1.5}Mn_{1.5}O_4$ spinel (Fig. 4b). This process is registered on the DTA curve with an exothermic effect having a maximum at 540°C (Fig. 2b).

$Cu_xMn_{1-x}(HCOO)_2 \cdot 2H_2O$ mixed crystals ($0.08 < x \leq 0.5$) dehydrate at about 130°C, and their decompositions are complete at 300°C (Fig. 2c–f). Our X-ray measurements show that the decomposition occurs with the formation of a two-phase system: oxides having a spinel structure and oxides having a structure of Mn_5O_8. It is known that the copper content in the $Cu_xMn_{3-x}O_4$ cubic spinel influences considerably on the values of the lattice parameter (14). However, our calculations show that the lattice parameters of the oxides obtained do not change with the change in the chemical compositions of the initial mixed formate crystals. One oxide phase retains the lattice parameters of $Cu_{0.4}Mn_{1.6}Mn_3O_8$, and the other retains the lattice parameters of the $Cu_{1.5}Mn_{1.5}O_4$ cubic spinel ($a = 8.279(2)$ Å). On the basis of our X-ray calculations we propose the following scheme of decompositions of the mixed crystals with $x > 0.08$:

$$Cu_xMn_{1-x}(HCOO)_2 \cdot 2H_2O \rightarrow aCu_{0.4}Mn_{1.6}Mn_3O_8 + bCu_{1.5}Mn_{1.5}O_4.$$

The increase in the x values leads to the increases in the coefficient b, and when $x = 0.5$, only a homogeneous solid phase having a spinel structure is produced (Fig. 3f).

$Cu_{0.4}Mn_{1.6}Mn_3O_8$ obtained according to the scheme above transforms into a two-phase system with α-Mn_2O_3 and $Cu_{1.5}Mn_{1.5}O_4$ at temperatures higher than 600°C. This process is registered on the DTA curves with exothermic effects at 540°C (Fig. 2c–e). In the case of the $Cu_{0.5}Mn_{0.5}(HCOO)_2 \cdot 2H_2O$ mixed crystal the exothermic effect at 540°C disappears completely (Fig. 2f), which confirms the claim that the spinel structure is formed at 300°C.

The formation of $Cu_{0.4}Mn_{1.6}Mn_3O_8$ mixed oxide calls for some additional comments: The monoclinic crystal structure of Mn_5O_8 consists of pseudohexagonal Mn^{4+} sheets with similar oxygen sheets on either side, giving a distorted octahedral coordination to the Mn^{4+}. The Mn^{2+} obtains an uncommon coordination from six oxygens forming a distorted trigonal prism (12). The existence of Mn^{2+} supposes the possibility of the formation of mixed oxides with a formula ($Me_x^{2+}Mn_{2-x}^{2+}Mn_3^{4+}O_8$) by replacement of the Mn^{2+} with other bivalent metals. Indeed, the crystal structures of the cadmium, cobalt, zinc, and copper analogues have been reported (12, 15, 16). While the crystal structure of $Cd_2Mn_3O_8$ is completely similar to that of

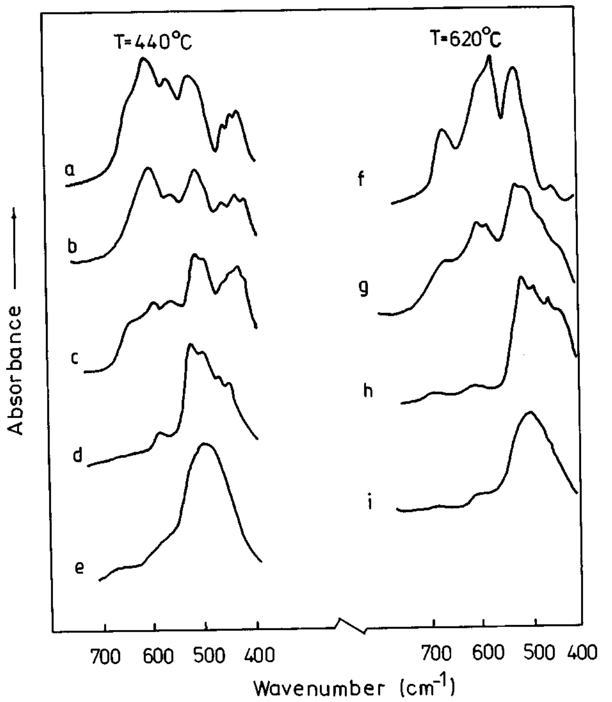

FIG. 5. Infrared spectra of the oxides obtained at 440 and 620°C: Mn_5O_8 (a); $Cu_{0.4}Mn_{1.6}Mn_3O_8$ (b); $Cu_{0.4}Mn_3O_8 + Cu_{1.5}Mn_{1.5}O_4$ (0.54 : 1) (c); $Cu_{1.5}Mn_{1.5}O_4$ "ordered" (d); $Cu_{1.5}Mn_{1.5}O_4$ "disordered" (e); α-Mn_2O_3 (f); α-$Mn_2O_3 + Cu_{1.5}Mn_{1.5}O_4$ (1 : 1) (g); α-$Mn_2O_3 + Cu_{1.5}Mn_{1.5}O_4$ (1 : 4.1) (h); $Cu_{1.27}Mn_{1.73}O_4$ "disordered" (i).

Mn_3O_8 (it means that all Mn^{2+} ions are replaced by Cd^{2+} ions), the crystal structures of the other analogues are quite different. Two types of Co^{2+} and Zn^{2+} ions, coordinated tetrahedrally and octahedrally by oxygen atoms, exist in the $Co_2Mn_3O_8$ and $Zn_2Mn_3O_8$ crystal structures (15). In the $Cu_2Mn_3O_8$ structure, however, the Cu^{2+} are surrounded by five oxygen atoms (16). The incorporation of a small amount of Cu^{2+} ions in the Mn_3O_8 structure will lead to a distortion of the Mn^{2+} polyhedra (Jahn–Teller effect), and as a result of this distortion the crystal structure becomes unstable. This fact explains the formation of a mixed oxide with formula $Cu_{0.4}Mn_{1.6}Mn_3O_8$ containing 6.26 at.% copper (only 1/5 of the Mn^{2+} ions are replaced by the copper ions) under the conditions of our experiments, irrespective of the composition of the mixed formate crystals.

The charge distribution of Cu and Mn in spinels has an influence on the IR spectra (17). The 1 : 3 ordering of the ions on the B-sublattice reduces the space group from O_h^7 to O^7, and according to White *et al.* (18) the number of IR active modes increases from 4 to 21. The spectra of the oxides obtained at 440 and 620°C are shown in Fig. 5. The spectrum of $Cu_{1.5}Mn_{1.5}O_4$ spinel obtained from the sample $Cu_{0.5}Mn_{0.5}(HCOO)_2 \cdot 2H_2O$ under different conditions: slowly cooled sample ("ordered" spinel) and quenched in water ("disordered" spinel) are shown in Figs. 5d and 5e, respectively. It is seen that only the slowly cooled specimen shows a fine structure in the IR spectrum, and the cation valences in $Cu_{1.5}Mn_{1.5}O_4$ have to be $Cu^+[Cu^{2+}_{0.5}Mn^{4+}_{1.5}]O_4$.

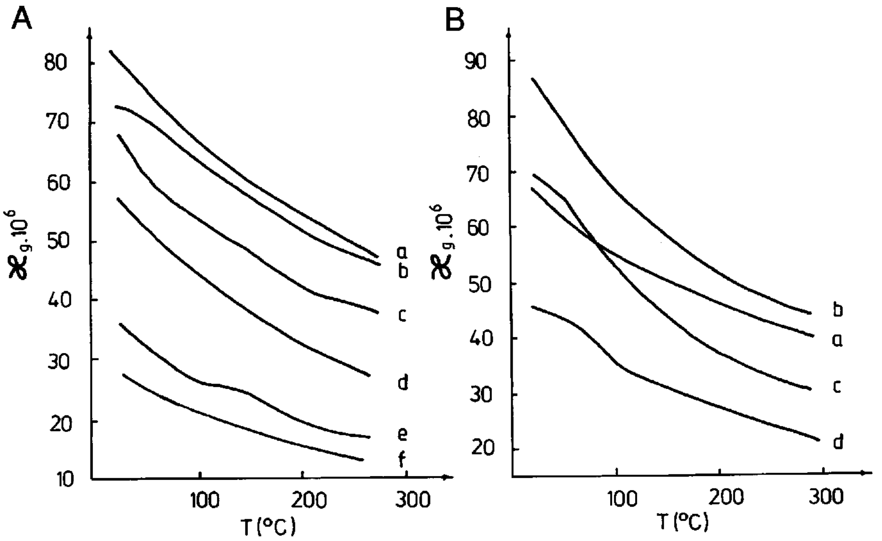

FIG. 6. Magnetic susceptibilities versus temperature. (A) Samples obtained at 440°C: Mn_5O_8 (a); $Cu_{0.4}Mn_{1.6}Mn_3O_8$ (b); $Cu_{0.4}Mn_{1.6}Mn_3O_8 + Cu_{1.5}Mn_{1.5}O_4$ (1 : 0.33) (c); $Cu_{0.4}Mn_{1.6}Mn_3O_8 + Cu_{1.5}Mn_{1.5}O_4$ (0.54 : 1) (d); $Cu_{0.4}Mn_{1.6}Mn_3O_8 + Cu_{1.5}Mn_{1.5}O_4$ (0.12 : 1) (e); $Cu_{1.5}Mn_{1.5}O_4$ (f): (B) Samples obtained at 620°C: α-Mn_2O_3 (a); α-$Mn_2O_3 + Cu_{1.5}Mn_{1.5}O_4$ (1 : 0.28) (b); α-$Mn_2O_3 + Cu_{1.5}Mn_{1.5}O_4$ (1 : 1) (c); α-$Mn_2O_3 + Cu_{1.5}Mn_{1.5}O_4$ (1 : 4.1) (d).

TABLE 2
Magnetic Moments of the Oxide Samples ("Ordered") Obtained at 440°C

Samples	θ (K)[a]	μ_{eff}(BM)		
	exp	exp	theor	exp
$Mn(HCOO)_2 \cdot 2H_2O \rightarrow 0.2Mn_5O_8 + Mn_2^{2+}Mn_3^{+}O_8$	– 118	10.1	10.2	—
$Cu_{0.08}Mn_{0.92}(HCOO)_2 \cdot 2H_2O \rightarrow 0.2Cu_{0.4}^{2+}Mn_{1.6}^{2+}Mn_3^{4+}O_8$	– 45	9.6	9.6	—
$Cu_{0.15}Mn_{0.85}(HCOO)_2 \cdot 2H_2O \rightarrow 0.17Cu_{0.4}Mn_{4.6}O_8 + 0.06Cu_{1.5}Mn_{1.5}O_4$	– 63	9.6	9.6	9.84
$Cu_{0.30}Mn_{0.70}(HCOO)_2 \cdot 2H_2O \rightarrow 0.1Cu_{0.4}Mn_{4.6}O_8 + 0.18Cu_{1.5}Mn_{1.5}O_4$	76	7.0	8.2	7.92
$Cu_{0.43}Mn_{0.57}(HCOO)_2 \cdot 2H_2O \rightarrow 0.03Cu_{0.4}Mn_{4.6}O_8 + 0.28Cu_{1.5}Mn_{1.5}O_4$	77	4.4	5.3	4.86
$0.33Cu_{0.5}Mn_{0.5}(HCOO)_2 \cdot 2H_2O \rightarrow Cu^+[Cu_{0.5}^{2+}Mn_{1.5}^{4+}]O_4$	74	3.6	4.1	—

[a] Curie–Weiss temperatures.

The sample $Cu_{0.43}Mn_{0.57}(HCOO)_2 \cdot 2H_2O$ also forms a $Cu_{1.27}Mn_{1.73}O_4$ homogeneous spinel phase after the decomposition of 600°C and quenching in water. The IR spectrum shows that a "disordered" spinel is obtained (Fig. 5i). The lattice parameter has a value of $a = 8.313(2)$ Å (Fig. 4e′). The slowly cooled specimen shows a fine structure in the IR spectrum (Fig. 5h) and the X-ray measurements indicate the formation of a two-phase system (Fig. 4e). The other formate samples could form $Cu_xMn_{3-x}O_4$ (where $x < 1$) homogeneous spinel phases under harder conditions (heating to temperature above 900–1000°C, then cooling at 700–800°C, and quenching in water), according to the scheme given in (14, 19).

Both the compositions and cation distributions in the oxide systems obtained are confirmed by magnetic measurements and calculations. The χ versus T curves are shown in Fig. 6. It is seen from the figure that the oxide samples are paramagnetic and that the χ values decrease with the increase in the temperature. The $1/\chi$–T curve obeys the Curie–Weiss law, and the calculated correlation coefficients have values of $R \geq 0.9930$. Because of the complicated type of the samples (heterogeneous oxide systems, two transition metals in different oxidation states), the magnetic moments were calculated for a given molecular mass. The experimental magnetic moments of the samples are given in the second columns of Tables 2 and 3. The theoretical magnetic moments were calculated as well. Taking into consideration both the type and strength of the crystal field, the following values of the magnetic moments of the ions were used for the calculations: $\mu_{eff}(Cu^{2+}) = 2.3$ BM; $\mu_{eff}(Mn^{2+}) = 5.92$ BM; $\mu_{eff}(Mn^{4+}) = 3.34$ BM in the case of the homogeneous samples Mn_5O_8 and $Cu_{0.4}Mn_{4.6}O_8$; $\mu_{eff}(Cu^{2+}) = 2.01$ BM; and $\mu_{eff}(Mn^{4+}) = 3.16$ BM in the case of the spinel phase (20, 21). The theoretical magnetic moments for the heterogeneous oxide samples were calculated taking into account the molar ratio of the oxides obtained.

The experimental magnetic moments coincide well with the theoretical ones in the case of the homogeneous samples (see Table 2). The experimental magnetic moment of the $Cu^+[Cu_{0.5}^{2+}Mn_{1.5}^{4+}]O_4$ spinel has a lower value than the theoretical one which is probably due to the exchange interactions and coincides well with that given in ref. (22). The oxide systems obtained from $Cu_xMn_{1-x}(HCOO)_2 \cdot 2H_2O$ mixed crystals (where $0.09 < x < 0.5$) show differences in the theoretical and experimental data (Table 2) because of the higher inaccuracy when the magnetic moments of two-phase systems are determined. For example, the $1/\chi$–T curve for the sample $Cu_{2.08}Mn_{2.98}O_8$ has a correlation coefficient of 0.98. The theoretical magnetic moments of the heterogeneous samples calculated on the

TABLE 3
Magnetic Moments of the Oxide Samples ("Ordered") Obtained at 620°C

Samples	θ (K)[a]	μ_{eff}(BM)	
	exp	exp	theor
$Mn(HCOO)_2 \cdot 2H_2O \rightarrow 0.5\alpha\text{-}Mn_2O_3$	– 109	5.8	6.7
$Cu_{0.15}Mn_{0.85}(HCOO)_2 \cdot 2H_2O \rightarrow 0.35\alpha\text{-}Mn_2O_3 + 0.1Cu_{1.5}Mn_{1.5}O_4$	26	6.5	6.0
$Cu_{0.30}Mn_{0.70}(HCOO)_2 \cdot 2H_2O \rightarrow 0.2\alpha\text{-}Mn_2O_3 + 0.2Cu_{1.5}Mn_{1.5}O_4$	102	6.7	6.7
$Cu_{0.43}Mn_{0.57}(HCOO)_2 \cdot 2H_2O \rightarrow 0.07\alpha\text{-}Mn_2O_3 + 0.29Cu_{1.5}Mn_{1.5}O_4$	57	10.2	9.2

[a] Curie–Weiss temperatures.

basis of the experimental data of $Cu_{0.4}Mn_{1.6}Mn_3O_8$ and $Cu_{1.5}Mn_{1.5}O_4$ are given in the last column of Table 2. For the samples prepared at 620°C see Table 3. The magnetic measurements confirm the claim that α-Mn_2O_3 and $Cu_{1.5}Mn_{1.5}O_4$ are formed as a result of the decomposition of the formates at 600°C.

ACKNOWLEDGMENTS

This work was supported by the Bulgarian National Foundation of Sciences under Project Ch 541. D.S. is indebted to the Alexander von Humboldt Foundation for a donation of the Fourier transform infrared spectrometer.

REFERENCES

1. F. Kapteijn, A. Dick van Langeveld, J. Moulijn, A. Andreini, M. Vuurman, A. Turek, J. Jehng, and I. Wachs, *J. Catal.* **150,** 94 (1994).
2. F. Kapteijn, L. Singoredjo, M. van Driel, A. Andreini, J. Moulijn, G. Ramis, and G. Busca, *J. Catal.* **150,** 105 (1994).
3. D. Stoilova, St. Peter, and H. D. Lutz, *Z. Anorg. Allg. Chem.* **620,** 1973 (1994).
4. D. Stoilova, *J. Solid State Chem.* **104,** 404 (1993).
5. J. Haber, J. Deren, and J. Sloczynski, *J. Chem. Anal.* (*Warszawa*) **6,** 659 (1961).
6. J. Deren, J. Haber, and J. Sloszynski, *Bull. Acad. Pol. Sci., Ser. Chim.* **9,** 659 (1961).
7. G. Bliznakov, D. Mehandjiev, and F. Elazorova, *C. R. Acad. Bulg. Sci.* **19,** 385 (1966).
8. J. Masuda and S. Shishido, *Thermochim. Acta* **28,** 377 (1979).
9. I. V. Archangelskii, L. N. Komissarova, and V. R. Falikman, *Coord. Chem.* **3,** 385 (1977).
10. D. Dollimore and K. H. Tonge, *J. Inorg. Nucl. Chem.* **29,** 621 (1967).
11. P. Baraldi, *Spectrochim. Acta A* **35,** 1003 (1979).
12. H. R. Oswald and M. J. Wampetich, *Helv. Chim. Acta* **50,** 2023 (1967).
13. W. Hase, *Phys. Status Solidi* **3,** K449 (1963).
14. R. E. Vandenberghe, G. G. Robbrecht, and V. A. M. Brabers, *Mater. Res. Bull.* **8,** 571 (1973).
15. A. Riou and A. Lecerf, *Acta Crystallogr. B* **31,** 2487 (1975).
16. A. Riou and A. Lecerf, *Acta Crystallogr. B* **33,** 1896 (1977).
17. V. A. M. Brabers and R. E. Vandenberghe, *Phys. Lett. A* **44,** 493 (1973).
18. W. B. White and B. A. De Angelis, *Spectrochim. Acta A* **23,** 985 (1967).
19. F. C. M. Driessens and G. D. Rieck, *Z. Anorg. Allg. Chem.* **351,** 48 (1967).
20. D. Mehandjiev and S. Angelov, "Magnetochemistry of Solid State," pp 67, 135, Nauka i Iskustvo, Sofia, 1979.
21. F. E. Mabbs and D. J. Machin, "Magnetism and Transition Metal Complexes," p. 63. Chapman and Hall, London, 1973.
22. R. E. Vandenberghe, G. G. Robbrecht, and V. A. M. Brabers, *Phys. Status Solidi* **34,** 583 (1976).